A New Parameter Extraction Technique for Small-Signal Equivalent Circuit of Polysilicon Emitter Bipolar Transistors

Seonghearn Lee, *Member, IEEE*, Byung R. Ryum, and Sang Won Kang

***Abstract*—We propose a new parameter extraction method for advanced polysilicon emitter bipolar transistors. This method is based on the predetermination of equivalent circuit parameters using the analytical expressions of de-embedded Z parameters of these devices. These parameter values are used as initial values for the parameter extraction process using optimization. The entire device equivalent circuit, containing RF probe pad and interconnection circuit parameters extracted by test structures, is optimized to fit measured S parameters for eliminating de-embedding errors due to the imperfection of pad and interconnection test structures. The equivalent circuit determined by this method shows excellent agreement with the measured S parameters from 0.1 to 26.5 GHz.**

I. Introduction

POLYSILICON emitter bipolar transistors have emerged as popular devices in high speed digital and analog circuit applications. They offer the advantages of improving current gain and forming extremely narrow bases. For the realization of high speed circuits, the popularity of these devices has been accelerated by the recent progress of a double polysilicon self-aligned process [1], [2]. An accurate small-signal equivalent circuit model for polysilicon self-aligned (PSA) bipolar transistors is a very useful tool for the high frequency circuit simulations. The equivalent circuit model can be used to optimize the microwave performance of the PSA bipolar transistors for efficient circuit designs.

In general, equivalent circuit parameters are extracted by fitting circuit parameter values to the measured device S parameters. However, the optimized parameter values during this fitting process may vary depending on the initial values and may deviate considerably from physical values, because of the large number of unknown variables in the equivalent circuit [3]. In order to obtain a global minimum result, it is essential to provide physically estimated initial values that may be determined from independent dc and RF measurements [3]. For the determination of initial values, the device resistances are usually estimated from I-V data [4], [5], and device capacitances are obtained from C-V measurement. Sometimes, the initial values are calculated approximately by simple theoretical equations using layer and layout parameters [6]. However, measured initial values may be different from the actual values in the equivalent circuit, due to the following reasons: 1) Since I-V data should be measured at high current level for extracting parasitic resistances, the measured values have uncertainties associated with high current effects [7]. 2) The C-V data measured in the frequency range of 1 to 100 MHz are not sensitive enough to accurately determine low capacitance values for advanced high speed devices. Therefore, it is better to determine initial values for resistances at the same current level as a bias of the small-signal circuit model, and to determine the capacitances in the high frequency range of GHz. The best method to achieve this is to extract initial values directly from the measured S parameters. Since RF probe pads and related interconnections add parasitics to the measured S parameters, these parasitics should be subtracted, that is, de-embedded, from the measured S parameters using the de-embedding technique [8], [9].

In this paper, we developed a new parameter extraction method based on the predetermination of device resistances and capacitances using analytical formulations of Z parameters derived from measured S parameters for the equivalent circuit model of PSA bipolar transistors. This expedites the extraction process, and results in better convergence during optimization. This new method does not require any other independent measurements or special test structures to determine device resistances and capacitances of the PSA bipolar transistors. Possible de-embedding errors are eliminated by optimizing the equivalent circuit of the PSA devices including RF probe-pattern (RF probe pad and interconnection) to fit the measured S parameters.

II. De-Embedding Procedure

Fig. 1(a) shows the layout of a typical RF probe-pattern used to measure the PSA bipolar transistors. Since this probe-pattern contains additional parasitics including resistances, inductances, and capacitances of pads and interconnects, an accurate de-embedding technique should be performed prior to the extraction of device parameters. The RF probe-pattern parasitics are subtracted from measured S parameters using four test structures. The first is the "open" structure that consists of RF probe pads and interconnections without contacting to device active area. The "short1," "short2," and "through" test structures consist of the "open" structure except with shorted base and emitter (B-E), shorted collector and emitter (C-E), and shorted base and collector (B-C) interconnections

Manuscript received April 3, 1993; revised October 12, 1993. The review of this paper was accepted by Associate Editor P. J. Zdebel.

The authors are with Semiconductor Devices Research Division, Electronics and Telecommunications Research Institute, Daejeon, 305-606, Korea.

IEEE Log Number 921446.

0018-9383/94$04.00 © 1994 IEEE

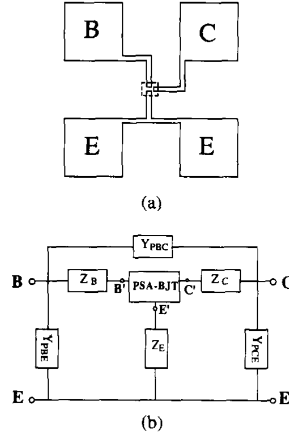

Fig. 1. (a) The schematic layout of a RF probe-pattern used for "on wafer" measurements for PSA bipolar transistors. The dashed box represents the device. (b) The physical equivalent circuit diagram representing the probe pattern.

at the plane of PSA bipolar transistors, respectively. Our de-embedding method becomes accurate, because these test structures are fabricated by the same process as the actual device except for skipping the interconnection contact process. Fig. 1(b) shows the physical equivalent circuit representation of the RF probe-pattern used for our de-embedding procedure. This consists of three parallel elements ($Y_{\rm PBE}$, $Y_{\rm PBC}$, $Y_{\rm PCE}$) and three series elements (Z_B, Z_E, Z_C).

High-frequency S-parameter measurements were performed on each test structures and several n-p-n double polysilicon self-aligned bipolar transistors with emitter area of 2×4 μm^2. The tests were performed at $I_c = 2.0$ mA and $V_{\rm CE} = 2$ V using Cascade Microtech RF probes and an HP8510B Network Analyzer for the frequency range of 0.1 to 26.5 GHz. The extraction of the PSA device parameters is performed by using de-embedded Z parameters after the probe-pattern parasitics are accurately removed. Note that the symbols used in this de-embedding procedure are defined in Table I. This procedure is summarized as follows:

(1) convert the measured S parameters $[S_O]$, $[S_{S1}]$, $[S_{S2}]$, and $[S_T]$ of "open," "short1," "short2," and "through" structures to each Y parameters $[Y_O]$, $[Y_{S1}]$, $[Y_{S2}]$, and $[Y_T]$, where $[Y_O]$ is expressed by parallel elements in Fig. 1(b) as follows:

$$[Y_O] = \begin{bmatrix} Y_{\rm PBE} + Y_{\rm PBC} & -Y_{\rm PBC} \\ -Y_{\rm PBC} & Y_{\rm PCE} + Y_{\rm PBC} \end{bmatrix}$$

(2) subtract $Y_{\rm PBE}$, $Y_{\rm PBC}$, $Y_{\rm PCE}$ from the $[Y_{S1}]$, $[Y_{S2}]$, and $[Y_T]$

$$[Y_{S1A}] = [Y_{S1}] - [Y_O]$$
$$[Y_{S2A}] = [Y_{S2}] - [Y_O]$$
$$[Y_{TA}] = [Y_T] - [Y_O]$$

(3) convert the $[Y_{S1A}]$ and $[Y_{S2A}]$ to $[Z_{S1}]$ and $[Z_{S2}]$

TABLE I
THE SYMBOL DEFINITIONS FOR THE DE-EMBEDDING PROCEDURE OF RF PROBE-PATTERN

Symbol	Definition
$[S_O]$	Measured S parameters of "open" structures
$[S_{S1}]$	Measured S parameters of "short1" structures
$[S_{S2}]$	Measured S parameters of "short2" structures
$[S_T]$	Measured S parameters of "through" structures
$[S_D]$	Measured S parameters of PSA bipolar transistors
$[Y_O]$	Measured Y parameters of "open" structures
$[Y_{S1}]$	Measured Y parameters of "short1" structures
$[Y_{S2}]$	Measured Y parameters of "short2" structures
$[Y_T]$	Measured Y parameters of "through" structures
$[Y_D]$	Measured Y parameters of PSA bipolar transistors
$[Y_{S1A}]$	$= [Y_{S1}] - [Y_O]$
$[Y_{S2A}]$	$= [Y_{S2}] - [Y_O]$
$[Y_{TA}]$	$= [Y_T] - [Y_O] = \begin{bmatrix} Y_{11TA} & Y_{12TA} \\ Y_{21TA} & Y_{22TA} \end{bmatrix}$
$[Y_{DA}]$	$= [Y_D] - [Y_O]$
$[Z_{S1}]$	$= \begin{bmatrix} Z_{11S1} & Z_{12S1} \\ Z_{21S1} & Z_{22S1} \end{bmatrix}$, Z parameters converted from $[Y_{S1A}]$
$[Z_{S2}]$	$= \begin{bmatrix} Z_{11S2} & Z_{12S2} \\ Z_{21S2} & Z_{22S2} \end{bmatrix}$, Z parameters converted from $[Y_{S2A}]$
$[Z_D]$	$= \begin{bmatrix} Z_{11D} & Z_{12D} \\ Z_{21D} & Z_{22D} \end{bmatrix}$, Z parameters converted from $[Y_{DA}]$
$[Z]$	$= \begin{bmatrix} Z_{11} & Z_{12} \\ Z_{21} & Z_{22} \end{bmatrix}$, de-embedded Z parameters of devices

(4) express Z_B, Z_E, and Z_C of RF probe-pattern model using $[Z_{S1}]$, $[Z_{S2}]$, and $[Z_T]$

$$Z_B + Z_E = Z_{11S1}$$
$$Z_E = \frac{1}{2}\left(Z_{11S1} + Z_{22S2} + \frac{1}{Y_{12TA}}\right)$$
$$Z_C + Z_E = Z_{22S2}$$

(5) convert the measured S parameters $[S_D]$ of PSA bipolar transistor to Y parameters $[Y_D]$

(6) subtract $Y_{\rm PBE}$, $Y_{\rm PBC}$, and $Y_{\rm PBC}$ from Y parameters $[Y_D]$

$$[Y_{\rm DA}] = [Y_D] - [Y_O]$$

(7) convert the Y parameters $[Y_{\rm DA}]$ to Z parameters $[Z_D]$

(8) subtract all series elements Z_B, Z_E, and Z_C of RF probe-pattern model from $[Z_D]$

$$Z_{11} = Z_{11D} - Z_{11S1}$$
$$Z_{12} = Z_{12D} - \frac{1}{2}\left(Z_{11S1} + Z_{22S2} + \frac{1}{Y_{12TA}}\right)$$
$$Z_{21} = Z_{21D} - \frac{1}{2}\left(Z_{11S1} + Z_{22S2} + \frac{1}{Y_{12TA}}\right)$$
$$Z_{22} = Z_{22D} - Z_{22S2}$$

III. DEVICE PARAMETER DETERMINATION

A hybrid-π small-signal equivalent circuit model for the PSA bipolar transistor without the RF probe-pattern is shown in Fig. 2(a). In this model, C_π is the emitter-base capacitance, r_π is the dynamic emitter resistance, $C_{\rm cc}$ is the base-collector junction capacitance, $r_{\rm bb}$ is the base resistance, $r_{\rm cc}$ is the collector resistance, $r_{\rm ee}$ is the emitter resistance including polysilicon resistance, and $C_{\rm cs}$ is the collector-substrate capacitance.

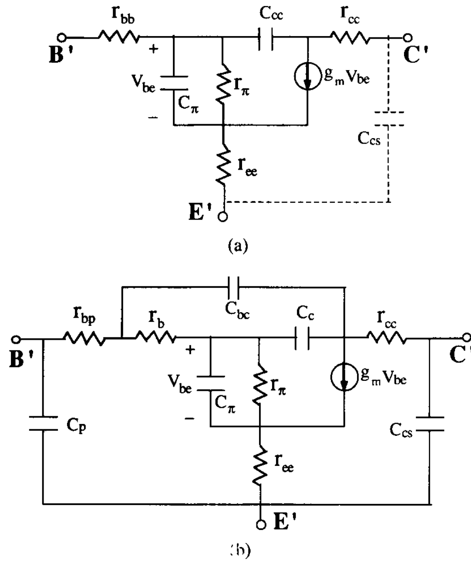

Fig. 2. (a) A small-signal hybrid-π equivalent circuit of PSA bipolar transistor. (b) Extended small-signal equivalent circuit of PSA bipolar transistor.

The small signal transconductance with transit time components is expressed as [10]

$$g_m = g_{mo}\exp(-j\omega\tau_d)$$

where $g_{mo}(= I_c/V_T)$ is the dc transconductance, and τ_d is the transit time phase delay of transconductance.

If the effect of $C_{\rm cs}$ is neglected in the low frequency region, this small-signal equivalent circuit is described by the following Z parameters:

$$Z_{11} = r_b + r_{\rm ee} + \frac{Z_\pi}{1+g_m Z_\pi} \tag{1}$$

$$Z_{12} = r_{\rm ee} + \frac{Z_\pi}{1+g_m Z_\pi} \tag{2}$$

$$Z_{21} = r_{\rm ee} + \frac{Z_\pi}{1+g_m Z_\pi}\left[1 - \frac{g_m}{j\omega C_{\rm cc}}\right] \tag{3}$$

$$Z_{22} = r_{\rm cc} + r_{\rm ee} + \frac{1}{j\omega C_{\rm cc}} + \frac{Z_\pi}{1+g_m Z_\pi}\left[1 - \frac{g_m}{j\omega C_{\rm cc}}\right], \tag{4}$$

where $Z_\pi = \frac{r_\pi}{1+j\omega r_\pi C_\pi}$. From the Z parameters, we can determine resistances and capacitance directly as follows:

$$r_{\rm bb} = {\rm Re}(Z_{11} - Z_{12}) \tag{5}$$

$$r_{\rm cc} = {\rm Re}(Z_{22} - Z_{21}) \tag{6}$$

$$C_{\rm cc} = -\frac{1}{\omega\,{\rm Im}(Z_{22} - Z_{21})}. \tag{7}$$

Taking the real part of $Z_{11} - Z_{12}$ for base resistance ($r_{\rm bb}$) removes the possible imaginary term due to capacitive effects [11]. Figs. 3 and 4 show the measured values used to extract $r_{\rm bb}$, $C_{\rm cc}$, $r_{\rm cc}$ and $r_{\rm ee}$. From the low-frequency values in Fig. 3, the value of $r_{\rm bb}$ is estimated to be 97Ω. The collector capacitance $C_{\rm cc}$ is determined to be about 0.095 pF from the values in the low frequency range, as shown in Fig. 4.

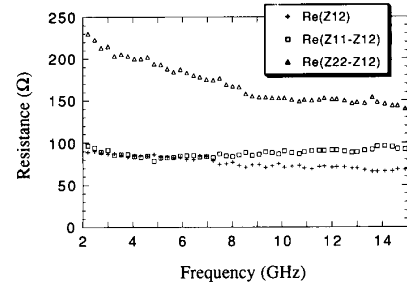

Fig. 3. Re (Z_{12}), Re (Z_{11}–Z_{12}), and Re (Z_{22}–Z_{12}) as a function of frequency.

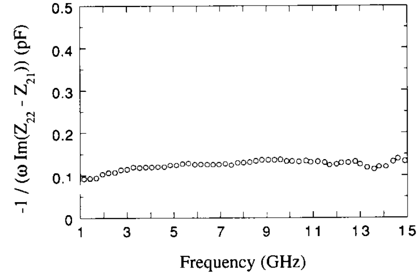

Fig. 4. $-1/[\omega\,{\rm Im}(Z_{22}–Z_{21})]$ as a function of frequency.

The value of $C_{\rm cs}$ is obtained from the high frequency region using the following equation:

$$C_{\rm cs} = \frac{1}{\omega}{\rm Im}\left[\frac{1}{Z'_{22}}\right] - \frac{1}{\omega}{\rm Im}\left[\frac{1}{Z_{22}}\right] \approx \frac{1}{\omega}{\rm Im}\left[\frac{1}{Z'_{22}}\right] - \frac{C_{\rm cc}}{1+\omega^2 C_{\rm cc}^2\left[r_{\rm cc} + r_{\rm ee} + \frac{g_m}{\omega^2 C_{\rm cc} C_\pi}\right]^2} \tag{8}$$

and $C_{\rm cs} \approx \frac{1}{\omega}{\rm Im}\left[\frac{1}{Z'_{22}}\right]$ in the frequencies that are high enough to neglect the second term in (8). The parameter Z'_{22} represents the parameter Z_{22} without neglecting $C_{\rm cs}$ and is the same as the de-embedded data. The $C_{\rm cs}$ value of around 20 fF is obtained from the uniform value in the high frequency region.

Note that (6) is not used to obtain collector resistance ($r_{\rm cc}$) because the measured data show unphysically large values of Re (Z_{21}) in the low frequency region. This may be explained by the following reason:

$$Z_{21} = \frac{2S_{21}}{(1-S_{11})(1-S_{22}) - S_{12}S_{21}} \tag{9}$$

and $Z_{21} \approx -2/S_{12}$ in the low frequency region [12]. The value of Z_{21} may fluctuate substantially, because S_{12} is small and subject to measurement error. Therefore, we use another equation given by

$$r_{\rm cc} = {\rm Re}\left[Z_{22} - Z_{12} - \frac{1}{j\omega C_{\rm cc}}\left(\frac{1}{1+g_m Z_\pi}\right)\right] = {\rm Re}[(Z'_{22} - Z'_{12})(1 + j\omega C_{\rm cs} Z_{22})] - \frac{g_m C_\pi}{C_{\rm cc}(g_m^2 + \omega^2 C_\pi^2)}. \tag{10}$$

In the high frequency region, the second term in (10) is neglected and Z_{22} is approximated by $r_{cc} + r_{ee} + \frac{1}{j\omega C_{cc}}$. Therefore, (10) is rewritten by

$$r_{cc} \approx \frac{\left[1 + \frac{C_{cs}}{C_{cc}}\right] \mathrm{Re}(Z'_{22} - Z'_{12}) - \omega r_{ee} C_{cs} \mathrm{Im}(Z'_{22} - Z'_{12})}{1 + \omega C_{cs} \mathrm{Im}(Z'_{22} - Z'_{12})}. \quad (11)$$

In order to use this approximation, the value of $\mathrm{Re}(Z'_{22} - Z'_{12})$ is roughly extracted by taking the uniform value in the high frequency region of Fig. 3. The value of $-\omega \, \mathrm{Im}\,(Z'_{22} - Z'_{12})$ is also obtained by taking the high-frequency values. Substituting these two values and the obtained values of C_{cc}, C_{cs}, and r_{ee}, the value of $r_{cc} \approx 235\ \Omega$ is roughly extracted.

Using (2), the emitter resistance in the low frequency region is given approximately by

$$r_{ee} \approx \mathrm{Re}(Z_{12}) - \frac{\alpha}{g_m} \quad (12)$$

where α is the common-base current gain. Since $g_m \approx 1/13$ and $\alpha \approx 1$, the value of $r_{ee} \approx 74\ \Omega$ is obtained from the low-frequency values of Re (Z_{12}) in Fig. 3.

IV. Parameter Extraction for RF Probe-Pattern Circuit Model

It has been pointed out that the errors associated with measuring and de-embedding S parameters results in large uncertainty in values of the equivalent circuit parameters obtained from post-extraction process [13]. The de-embedding errors are often caused by the process variation across the wafer, because the probe-pattern test structures are located at the different position. Also the test structures are not exactly the same as the real pads and interconnections, due to the extra inductances and resistances of aluminum lines in the "short" test pattern, and due to extra fringe capacitances in the "open" test pattern [14], [15]. Even small errors in the de-embedding process may lead to considerable errors in some of the extracted parameter values [13]. In order to reduce the uncertainty of the extracted values, the pad and interconnection parasitics are converted to an accurate equivalent circuit model, and the model parameters are allowed to vary within narrow bounds during the parameter optimization process [14], [15].

For this purpose, we develop a probe-pattern equivalent circuit model shown in Fig. 5. The RF probe pad is modeled as the lossy capacitance that consists of pad capacitance connected in series with a substrate resistance depending on the resistivity of p-bulk Si substrate [16], [17]. The interconnection is modeled by series connection of resistance and inductance. In general, most previous equivalent circuit modeling results have been optimized without independent measurements of pad and interconnection parasitics. This may produce unphysical parameter values during the optimization due to the large number of unknown parameters. Therefore, the RF probe-pattern parasitics must be predetermined with properly designed test structures [14].

To do this, the "open," "short1," and "short2" circuit model parameters are simultaneously optimized to fit the measured

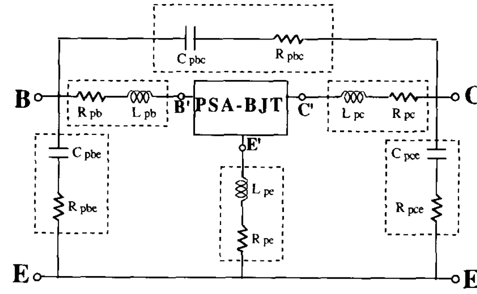

Fig. 5. A small-signal equivalent circuit model of RF probe-pattern.

S parameters using the E's of Touchstone computer-aided microwave optimization program [18]. Since all pad and interconnection parameters, excluding capacitances associated with open end gaps of emitter, base, and collector interconnect lines, should have the same values in all of the circuit models, these parameters are assigned as common variables in this optimization. Using this procedure, the following values were extracted for a probe-pattern model: $L_{pb} = 89$ pH, $L_{pc} = 92$ pH, $L_{pe} = 55$ pH, $R_{pb} = 12.3\ \Omega$, $R_{pc} = 5.6\ \Omega$, $R_{pe} = 1.1\ \Omega$, $R_{pbe} = 105\ \Omega$, $R_{pce} = 99\ \Omega$, $R_{pbc} = 166\ \Omega$, $C_{pbe} = 234$ fF, $C_{pce} = 255$ fF, and $C_{pbc} = 43$ fF. The simulated parameter $S11$ of "open" and "short1" circuit, and simulated parameter $S22$ of "open" and "short2" circuit, are compared with the measured parameters in Fig. 6. Reasonable agreement is seen between the circuit model simulations and the measured S parameters in the range of 0.1–26.5 GHz. Thus, the circuit in Fig. 5 is a realistic model for pad and interconnection structure of Si-based bipolar transistors. The extracted equivalent circuit of the RF probe-pattern may become valuable information to minimize the probe-pattern parasitics.

V. Optimization Procedure for Accurate Parameter Extraction

The above estimated values are now tuned to real data for the PSA bipolar transistor including probe-pattern parasitics. This process leads to more accurate and physical parameter extraction. An important factor to be considered to obtain good parameter extraction is that the equivalent circuit should be accurate enough to model a device under a test. In order to have a better curve-fitting to the measured S parameters, the base-collector RC distributed components [19] should be considered in the equivalent circuit for optimization. For these effects, r_{bb} and C_{cc} are divided into intrinsic (r_b, C_c) and extrinsic (r_{bp}, C_{bc}) sections, where r_{bp} is the extrinsic base resistance including $p+$ base polysilicon and contact area, and C_{bc} is the extrinsic base-collector junction capacitance under an extrinsic base area. Another capacitance (C_p) associated with silicon dioxide between base and emitter polysilicon layers is also inserted between the extrinsic base contact and emitter ground. The extended small-signal model including these components is shown in Fig. 2(b).

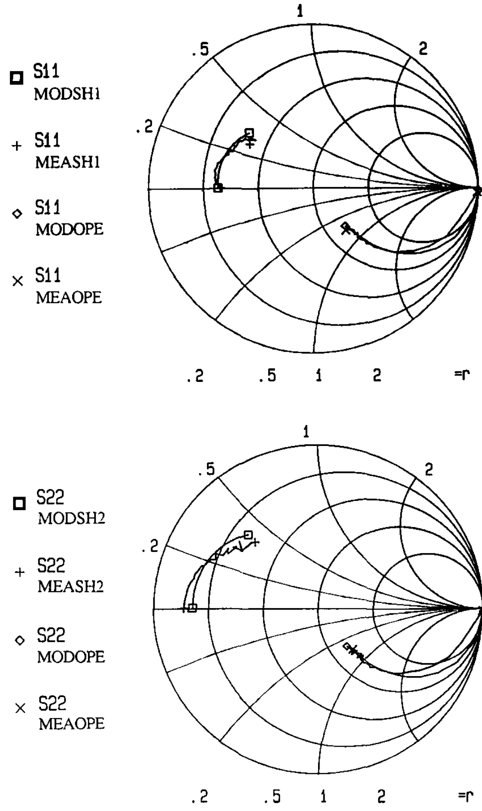

Fig. 6. Comparison between measured (MEAOPE, MEASH1) and modeled (MODOPE, MODSH1) parameter S_{11} of "open" and "short1" circuit test structures (upper circle), measured (MEAOPE, MEASH2) and modeled (MODOPE, MODSH2) parameter S_{22} of "open" and "short2" circuit test structures (lower circle), in the frequency range of 0.1 to 26.5 GHz.

In this case, initial values for C_c and $C_{\rm bc}$ are estimated by

$$C_c = \frac{C_{\rm cc}}{k}$$

$$C_{\rm bc} = \frac{(k-1)C_{\rm cc}}{k}$$

where $k(= A_b/A_e)$ is the area ratio between emitter and base regions.

The expression for base resistance is also modified by

$$r_{\rm bp} + \frac{r_b}{k} \approx {\rm Re}(Z_{11} - Z_{12}).$$

The $r_{\rm bp}$ term is roughly obtained by substituting the value of r_b calculated by simple theoretical equation [6] into the above equation.

The PSA bipolar transistor equivalent circuit with RF probe-pattern parasitics was optimized to obtain the closest possible fit to the measured S parameters. The values of all probe-pattern and PSA bipolar transistor elements obtained from our extraction method in Section III and IV are used as initial values, and permitted to vary within narrow bounds during this optimization. These initial values provide good starting position to obtain the actual global minimum results during the optimization. The extracted parameter values of the full equivalent circuit are listed in Table II. The model-produced S parameters of an entire equivalent circuit including device and probe-pattern are compared with measured S parameters, and show the excellent agreement in Fig. 7. Since initial parameter values obtained from analytical Z parameter equations are more physically acceptable, these values allow us to extract the PSA bipolar transistor parameters with greater accuracy.

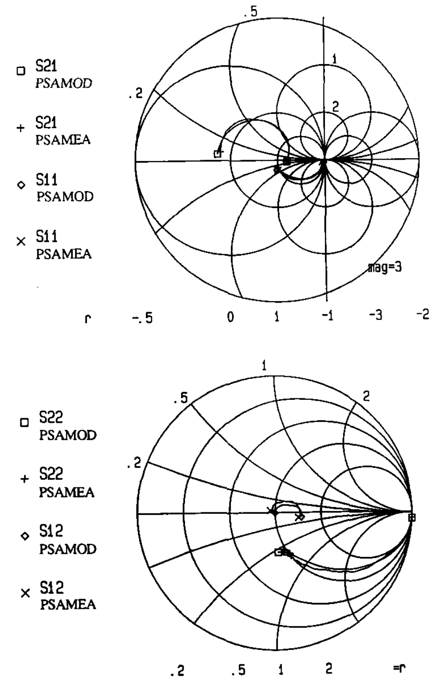

Fig. 7. Comparison between measured (PSAMEA) and modeled (PSAMOD) S-parameters of the PSA bipolar transistor including RF probe-pattern at I_c = 2.0 mA and $V_{\rm CE}$ = 2.0 V in the frequency of 0.1 to 26.5 GHz.

TABLE II
EXTRACTED SMALL-SIGNAL MODEL PARAMETERS OF A PSA BIPOLAR TRANSISTOR AND RF PROBE-PATTERN

L_{pb}	91 pH	r_π	863 Ω
L_{pc}	97 pH	r_b	168 Ω
L_{pe}	52 pH	r_{bp}	27 Ω
R_{pb}	11.6 Ω	r_{ee}	60 Ω
R_{pc}	5.1 Ω	r_{cc}	219 Ω
R_{pe}	1.0 Ω	C_π	0.95 pF
R_{pbe}	107 Ω	C_c	22 fF
R_{pce}	108 Ω	C_{bc}	71 fF
R_{pbc}	170 Ω	C_p	24 fF
C_{pbe}	214 fF	C_{cs}	30 fF
C_{pce}	265 fF	g_{mo}	79 mS
C_{pbc}	55 fF	τ_d	3.0 ps

VI. CONCLUSION

A new parameter extraction technique that uses predetermined Z parameter values as initial parameter values for optimization has been proposed. This technique results in faster extraction time and better convergence in the optimization process. In addition, this may increase the probability

of approaching a global minimum solution with a physical meaning. It also has the advantage that any additional measurements or test structures are not required to obtain physical device parameter values. Pad and interconnection parasitics are accurately determined by test structures before optimizing the equivalent circuit parameters. The de-embedding errors associated with the imperfection of test structures are removed by permitting probe-pattern parasitics to vary within narrow bounds during the optimization. The equivalent circuit of the PSA bipolar transistor extracted from our new method fits the measured S parameters very well up to 26.5 GHz.

ACKNOWLEDGMENT

The authors gratefully acknowledge the staff of the Advanced Bipolar Technology Research Group at ETRI for PSA bipolar transistor fabrication. They would like to thank H-S. Rhee for help with S parameter measurement, and Dr. Y. S. Ku for his helpful discussions and encouragement.

REFERENCES

[1] T. H. Ning, R. D. Isaac, P. M. Solomon, D. D-L. Tang, H-N. Yu, C. Feth, and S. K. Wiedmann, "Self-aligned bipolar transistors for high-performance and low-power delay VLSI," *IEEE Trans. Electron Dev.*, vol. ED-28, pp. 1010–1014, 1981.

[2] T. Sakai, S. Konaka, Y. Kobayashi, M. Suzuki, and Y. Kawai, "Gigabit logic bipolar technology: advanced super self-aligned process technology," *Electron. Lett.*, vol. 19, pp. 283–284, 1983.

[3] R. J. Trew, U. K. Mishra, and W. L. Pribble, "A parameter extraction technique for heterojunction bipolar transistors," *IEEE MTT-S Int. Microwave Symp. Dig.*, pp. 897–900, 1989.

[4] I. E. Getreu, *Modeling the Bipolar Transistor.* Amsterdam: Elsevier, 1978.

[5] T. H. Ning and D. D. Tang, "Method for determining the emitter and base series resistance of bipolar transistors," *IEEE Trans. Electron Dev.*, vol. 31, pp. 409–412, 1984.

[6] A. S. Grove, *Physics and Technology of Semiconductor Devices.* New York: Wiley, 1967.

[7] A. Neugroschel, "Measurement of the low-current base and emitter resistances of bipolar transistors," *IEEE Trans. Electron Dev.*, vol. 34, pp. 817–822, 1987.

[8] H. Cho and D. E. Burk, "A shree-step method for the de-embedding of high frequency S-parameter measurements," *IEEE Trans. Electron Dev.*, vol. 38, pp. 1371–1375, 1991.

[9] M. C. A. M. Koolen, J. A. M. Geelen, and M. P. J. G. Versleijen, "An improved de-embedding technique for on-wafer high-frequency characterization," *IEEE Bipolar Circuits and Technol. Meet.*, pp. 188–191, 1991.

[10] A. P. Laser and D. L. Pulfrey, "Reconciliation of methods for estimating f_{max} for microwave heterojunction transistors," *IEEE Trans. Electron Dev.*, vol. 38, pp. 1685–1692, 1991.

[11] H-S. Rhee, S. Lee, and B. R. Kim, "The analysis of dc and ac current crowding effects in high speed bipolar transistors with a new and accurate measurement technique," *Int. Semicond. Device Res. Symp.*, pp. 647–650, 1993.

[12] G. Gonzalez, *Microwave Transistor Amplifiers Analysis and Design.* Englewood Cliffs, NJ: Prentice-Hall, 1984, pp. 24–25.

[13] R. L. Vaitkus, "Uncertainty in the values of GaAs MESFET equivalent circuit elements extracted from measured two-port scattering parameters," *IEEE/Cornell Conf. on High Speed Semicond. Devices and Circuits*, 1983, pp. 301–308.

[14] S. Lee and A. Gopinath, "New circuit model for RF probe pads and interconnections for the extraction of HBT equivalent circuits," *IEEE Electron Device Lett.*, vol. 12, pp. 521–523, 1991.

[15] S. Lee and A. Gopinath, "Parameter extraction technique for HBT equivalent circuit using cutoff mode measurement," *IEEE Trans. Microwave Theory Tech.*, vol. 40, pp. 574–577, 1992.

[16] P. J. van Wijnen, H. R. Claessen, and E. A. Wolsheimer, "A new straightforward calibration and correction procedure for "On wafer" high frequency S-parameter measurements (45 MHz–18 GHz)," *IEEE Bipolar Circuits and Technology Meet.*, pp. 70–73, 1987.

[17] A. Fraser, R. Gleason, and E. W. Strid, "GHz on-silicon-wafer probing calibration methods," *IEEE Bipolar Circuits and Technology Meet.*, pp. 154–157, 1988.

[18] EEsof Touchstone Ref. Manual, version 1.7, EEsof Inc., 1989.

[19] W. M. C. Sansen and R. G. Meyer, "Characterization and measurement of the base and emitter resistances of bipolar transistor," *IEEE J. Solid-State Circuits*, vol. SC-7, pp. 492–498, Dec. 1972.

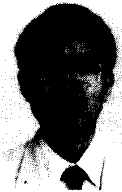

Seonghearn Lee was born in Junjoo, Korea, in 1962. He received the B. E. degree in electronic engineering in 1985 from Korea University, Seoul, Korea, and the M.S. and Ph.D. degrees in electrical engineering from the University of Minnesota, Minneapolis, MN, in 1989 and 1992, respectively.

In 1992, he joined the Semiconductor Devices Research Division at the Electronics and Telecommunications Research Institute, Daejon, Korea, where he has been a Senior Research Scientist. He is currently engaged in research on polysilicon emitter bipolar transistors and Si/SiGe heterojunction bipolar transistors.

Byung R. Ryum was born in Seoul, Korea, in 1959. He received the B.S. and M.S. degrees in electronic engineering from Seoul National University, Seoul, Korea, in 1982 and 1984, respectively, and the Ph.D. degree in electrical engineering from Northwestern University, Evanston, IL, in 1990.

Since 1990 he has been with the Semiconductor Devices Research Division at the Electronics and Telecommunications Research Institute, Daejon, Korea, where he is a Senior Research Scientist in charge of research and development of Si/SiGe heterojunction devices. His research interests include Si/SiGe epitaxy technology by MBE and CVD, modular process, process integration, design and modeling of exploratory Si/SiGe heterojunction bipolar transistors for high performance analog and digital IC's.

Sang Won Kang was born in Taegu, Korea, in 1952. He received the B.S. degree in Materials Science in 1976 from Seoul National University, Seoul, Korea, and the M.S. and Ph.D. degrees in electronic materials science from the Korean Advanced Institute of Science and Technology, Daejon, Korea, in 1978 and 1990, respectively.

Since 1978 he has been with the Semiconductor Devices Research Division at the Electronics and Telecommunications Research Institute, Daejon, Korea, where he is now a Fellow Research Scientist. From 1978 to 1985, he worked on Si epitaxy and unit process technology. Since 1986 he has been researching SiGe molecular beam epitaxy, heterojunction bipolar transistors, and SOI CMOS devices, as well as the development of Si process equipment, unit process, and micromachining related devices.